

NASA CR-66708

STUDY OF THE ASTRONAUT'S CAPABILITIES TO MAINTAIN
LIFE SUPPORT SYSTEMS AND CABIN HABITABILITY
IN WEIGHTLESS CONDITIONS

MOD 3

A NEW TECHNIQUE FOR INVESTIGATING CARGO TRANSFER
IN SIMULATED WEIGHTLESS ENVIRONMENTS

By Harry L. Loats, Jr. and G. Samuel Mattingly

Distribution of this report is provided in the interest of
information exchange. Responsibility for the contents
resides in the author or organization that prepared it

Prepared under Contract No. NAS1-7887 by
Environmental Research Associates
Randallstown, Maryland 21133

for



NATIONAL AERONAUTICS AND SPACE ADMINISTRATION

ERA 68-2

STUDY OF THE ASTRONAUT'S CAPABILITIES TO MAINTAIN
LIFE SUPPORT SYSTEMS AND CABIN HABITABILITY
IN WEIGHTLESS CONDITIONS

MOD 3

A NEW TECHNIQUE FOR INVESTIGATING CARGO TRANSFER
IN SIMULATED WEIGHTLESS ENVIRONMENTS

By Harry L. Loats, Jr. and G. Samuel Mattingly

Prepared Under Contract No. NAS1-7887 by
Environmental Research Associates
Randallstown, Maryland 21133

for

National Aeronautics and Space Administration
Langley Research Center
Hampton, Virginia

Otto F. Trout, Jr.
*NASA Project Engineer

CONTENTS

	Page
FIGURES	iv
TABLES	iv
SUMMARY	1
INTRODUCTION	1
DEVELOPMENT OF CARGO TRANSPORT SIMULATOR	2
Calibration of the Rotational Inertia Component and Simulator Configuration Determination	4
Theory of the (RIC)	5
Calibration of the Force Measurement Component	10
SIMULATOR CONFIGURATION	10
SIMULATION TECHNIQUE AND RESULTS	12
CONCLUSIONS AND RECOMMENDATIONS	19
SYMBOLS	23
APPENDIX A DETERMINATION OF THE OPERATIONAL CHARACTERISTICS OF THE RIC	24
APPENDIX B ANALYSIS OF FORCES FOR UW CARGO TRANSPORT SIMULATOR--LINEAR VERSION	28

FIGURES

	Page	
FIGURE 1	LINEAR VERSION OF THE CTS	2
FIGURE 2	PLATFORM SLOPE DETERMINATION	3
FIGURE 3	CTS--ROTARY VERSION	4
FIGURE 4	CALIBRATION SETUP FOR THE RIC	5
FIGURE 5	RIC	6
FIGURE 6	FORCE MEASUREMENT COMPONENT	11
FIGURE 7	CARGO TRANSPORT SIMULATOR SCHEMATIC	13
FIGURE 8	CARGO CONFIGURATIONS	13
FIGURE 9	MOTION ANALYSIS	16

TABLES

TABLE I	PACKAGE MASS - CONFIGURATION SUMMARY	14
TABLE II	RESULTS OF SIMULATION-SERIES 1	18
TABLE III	RESULTS OF SIMULATION-SERIES 2	18

A NEW TECHNIQUE FOR INVESTIGATING CARGO TRANSFER IN SIMULATED WEIGHTLESS ENVIRONMENTS

By Harry L. Loats, Jr. and G. Samuel Mattingly
Environmental Research Associates

SUMMARY

The following report describes a new technique for investigating cargo transfer in simulated weightless and altered gravity environments. The technique utilizes the water immersion simulation technique validated by Environmental Research Associates in the Gemini extravehicular simulation program to provide a neutrally buoyant medium for the subject.

A series of 18 evaluation runs was performed on the final version of the simulator, comprising 3 cargo package configurations and 3 package masses. A continuous 16 mm motion picture record at 24 fps was made to provide evaluation data. The cargo variations included package masses of 2, 6, and 10 slugs and cubical packages of 12, 17, and 21 in. linear dimension. Two series of 9 runs were accomplished to determine learning characteristics.

INTRODUCTION

Current plans for the activation and utilization of orbital space stations imply steadily increasing reliance on the astronaut's ability to transfer cargo to and thru sections of the spacecraft. The mass and configuration of these cargo packages cannot logically be specified until relatively late in the mission design phase unless rules and guidelines for cargo transfer can be established. The only means presently at hand to provide this necessary information is by simulation techniques. This report details the initial effort in establishing a new technique for simulating cargo transport, utilizing water immersion techniques. The technique derives from a proprietary concept generated by Environmental Research Associates. Patent proceedings have been initiated by Environmental Research Associates.

Conventional simulation techniques, utilizing water immersion in conjunction with cargo transfer, have suffered from the degradatory effects of water drag on the subject and cargo motion. The present technique simulates the motion of the cargo relative to the spacecraft structure without necessitating gross motion of the subject or the cargo. The subject and cargo package remain fixed while relative motion is simulated by the moving transfer

aid device. The cargo mass is simulated by a rotational inertia component and cable system which is located outside the water environment.

DEVELOPMENT OF CARGO TRANSPORT SIMULATOR

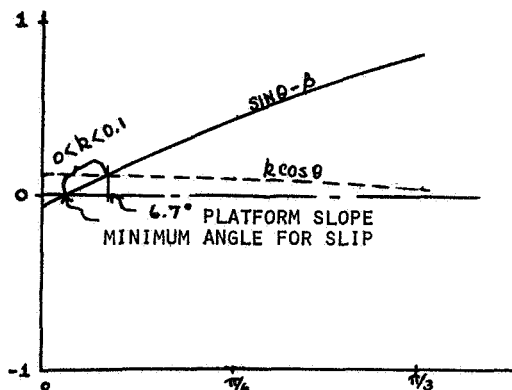
The initial version of the Cargo Transport Simulator was fabricated in the engineering office at Environmental Research Associates for the purpose of evaluating the operational characteristics of the simulator. During the first week of August 1968, a variety of sheaves and sheave positions were tested, using a spring scale to measure the system friction. The inertial mass was simulated by a loaded wheel cart pulled across an asphalt tile surface.

An initial full scale version of the simulator to be used in the water immersion mode was completed during the second week in August and fabricated during the third week. The simulator was constructed of aluminum extrusions and utilized V-belt sheaves with needle-bearing inserts, as shown in Figure 1. To overcome system friction, the load-bearing cart was placed on a sloping platform. Figure 2 depicts the graphical solution of the slope of the platform. The first test of the simulator in the water immersion mode was conducted August 19, 1968.



FIGURE 1 - LINEAR VERSION OF THE CTS

The simulated mass was restrained by a separate structure and the test subject was unrestrained. Masses up to 10 slugs were used



Friction Coef. $k = 0.1$

System Drag = 10#

Mass = 15.5 slugs

FIGURE 2 - PLATFORM SLOPE DETERMINATION

in the test runs. The test subject had no difficulty in accelerating or moving the masses. The utility of the tests, however, was limited due to the short distance of travel (66 in.) permitted by the mock-up design and by direction of motion considerations.

A significant modification was made to the simulator to include a rotary inertia component to replace the load-bearing cart. Tests were made of this modification on August 26, 1968. This version of the simulator allows for a continuous movement of the simulated mass by means of the endless cable loop. The cable was marked so that the test subject could identify starting and stopping positions. The tests of this version of the simulator were conducted with the subject unrestrained and the package restrained at its mass center.

In order to compensate for the drag of the system, an air motor was coupled to the idler sheave. Results indicated that the air motor technique was not adequate and that the restraint system used to hold the package did not produce the desired motions. During the last week in August and the first week in September, a modification was made to the drive system to include an electric

powered motor and to the restraint system to include a coupling technique between test subject and test package.

The final series of tests were performed September 9, 10, 11, 12, and 14. During this time, several versions of a restraint technique were evaluated, and the electric drive technique was tested and discarded in favor of a manual drive in which a technician assists the rope travel manually. The final version of the simulator was tested September 12, 1968. This included the manual assist for the drive system and a restraint technique in which the test subject was restrained by a harness in which the mass center of the system was approximately at the mass center of the subject-package combination. This version of the simulator is shown in Figure 3.

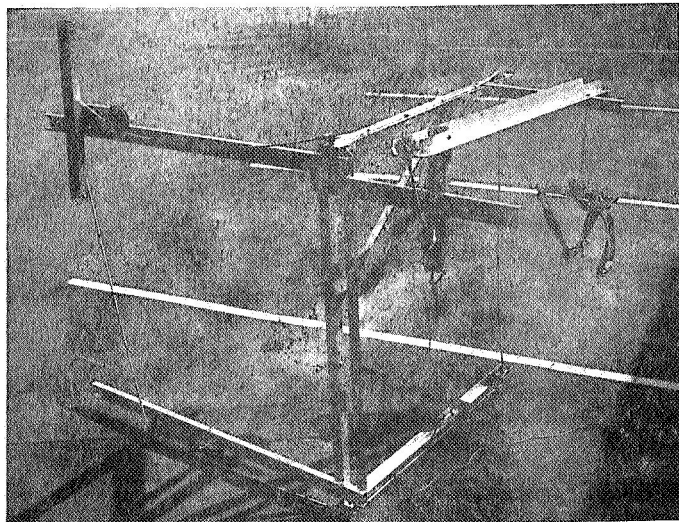


FIGURE 3 - CTS--ROTARY VERSION

Calibration of the Rotational Inertia Component
and Simulator Configuration Determination

The rotational inertia component (RIC) of the Cargo Transport Simulator (CTS) was calibrated by the following technique. A schematic representation of the calibration equipment is given in Figure 4.

Constant acceleration was provided by the gravitational force exerted on the reference mass acting directly on the drive drum. After added masses were symmetrically located on the support of

the rotational inertia component, the test run commenced by allowing the reference mass to drop under the influence of gravity.

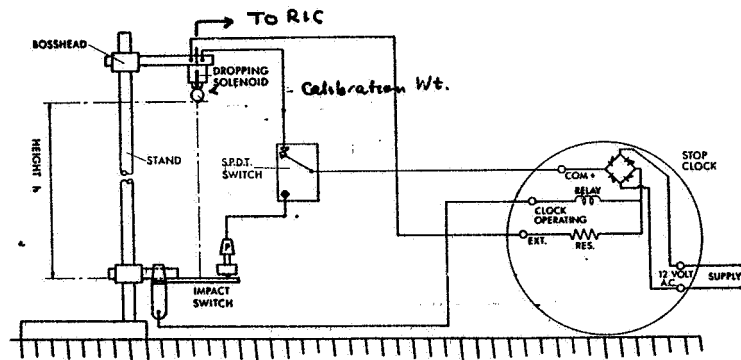


FIGURE 4 - CALIBRATION SETUP FOR THE RIC

Motion of the reference mass started by breaking the contact of the start-up disconnect, thus causing the timer circuit to be activated. Uniform angular acceleration of the (RIC) continued until the device had traveled approximately 355°. At this point, an opaque element located on one end of the (RIC) intercepted the photocell beam. This action deactivated the timing circuit. The time for a 355° rotation of the (RIC), under constant angular acceleration, was measured by this technique.

Theory of the (RIC)

For the pure dumbbell case (no consideration of the channel cross support.

Assuming

$$r_2 = r_1 = R; m_1 = m_2 = \frac{M}{2}$$

$$I = \frac{M}{2}(R^2 + R^2) = MR^2$$

The geometry of the (RIC) is given in Figure 5. Applying a tension

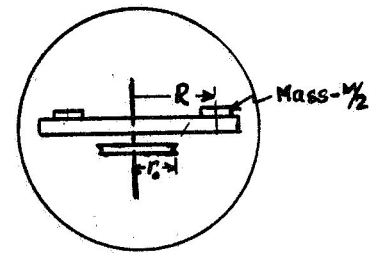
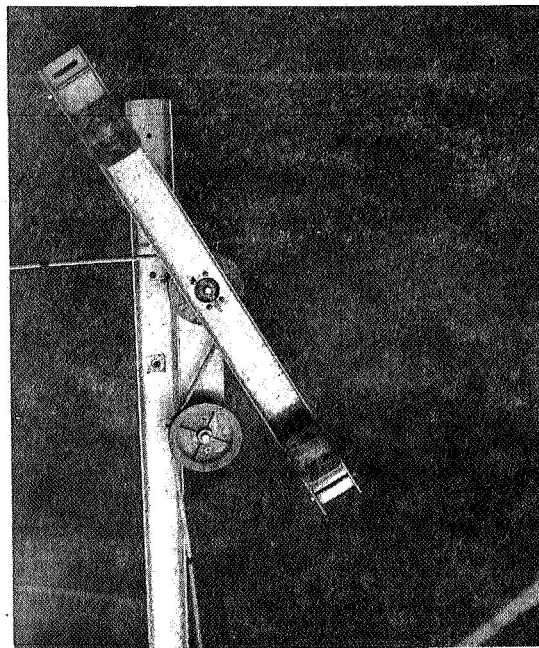


FIGURE 5 - RIC

to the cord around the drive pulley,

$$F \cdot r_o = I\alpha$$

with

$$\alpha = \frac{a_T}{r_o}$$

then

$$\frac{Fr_o^2}{a_\tau} = MR^2$$

Rearranging terms,

$$M = \frac{F}{a_\tau} \left(\frac{r_o}{R}\right)^2$$

Considering the motion characteristics of the simulated cargo,

$$\frac{F}{a_\tau} = m_s \equiv \text{mass of the simulated cargo package,}$$

$$\therefore M = m_s \left(\frac{r_o}{R}\right)^2$$

For the present case,

$$M = m_s \left(\frac{2}{12}\right)^2 = \left(\frac{1}{36}\right) m_s$$

In the actual case, the rotational inertia is composed of two factors; the contribution from the dumbbell and the contribution of the support member. The initial series of (RIC) calibration runs are summarized in Appendix A.

Since

$$Fr_o = I_T \alpha$$

Rearranging terms,

$$\frac{Fr_o^2}{a_\tau} = I_T = MR^2 + k$$

where k represents the constant contribution of the support member.

Solving for the variable mass M,

$$M = m_s \left(\frac{r_o}{R}\right)^2 - \frac{k}{R^2}$$

When $M = 0$, e.g., effect of the support member only,

$$m_s = \frac{k}{R^2} \frac{R^2}{r_o^2} = \frac{k}{r_o^2}$$

or

$$k = m_s r_o^2$$

This case was evaluated experimentally and the mass simulated was determined to be $m_s = 2.232$ slugs. Therefore, considering

$$m_s = 2.232 \text{ when } M = 0 \text{ and } r_o^2 = \frac{1}{36}$$

$$k = 0.06$$

The resulting relationship between the added mass M, the simulated mass m_s , and the centroid of the added mass R is given by

$$M = m_s \left(\frac{r_o}{R}\right)^2 - \frac{0.06}{R^2}$$

Using

$$R = 1.11, r_o = 2''$$

$$(M + 0.05) 43.5 = m_s$$

But, considering constant acceleration and homogeneous initial conditions,

$$m_{s_e} = \frac{Wt^2}{2.18}$$

The results of the experimental determination of m_{s_e} are given in Appendix A.

Combining the foregoing results and using the actual mass of subject 1 (5.28 slugs) and the actual dimension r_o ,

$$r_o = 2.063'' = \left(\frac{r_o}{R}\right)^2 = \frac{1}{33.834R^2}$$

Solving for k, and remembering

$$M = m_s \left(\frac{r_o}{R}\right)^2 - \frac{k}{R^2}$$

With

$$M = 0$$

$$m_s = \frac{k}{r_o^2} = \frac{F}{a_\tau}$$

From the experimental results,

$$a_\tau = 0.778$$

and

$$F = 2.25$$

$$\therefore m_s = 2.892$$

Substituting

$$r_o^2(2.892) = k$$

or

$$k = (2.892) \left(\frac{1}{33.834}\right) = 0.085$$

Substituting k into the formula for M,

$$M = \frac{m_s}{(33.834)R^2} - \frac{0.085}{R^2} = \frac{1}{R^2}(0.0296 m_s - 0.0855)$$

Now, $m_s = m_o + m_p$, where m_o is the subject mass and m_p is the package mass. For package masses of 2, 6, and 10 slugs,

$$m_{s_1} = 7.28$$

$$m_{s_2} = 11.28$$

$$m_{s_3} = 15.28$$

Arbitrarily selecting a constant $M = \frac{10}{32.2}$ slugs

$$M = \frac{10}{32.2} = \frac{1}{R^2} [(15.28)(0.0296) - 0.0855]$$

Solving for R_i

$$R_3 = [3.22 [15.28(0.0296) - 0.0855]]^{\frac{1}{2}} = 13.04''$$

$$R_2 = [3.22 [11.28(0.0296) - 0.0855]]^{\frac{1}{2}} = 10.73''$$

$$R_1 = [3.22 [7.28(0.0296) - 0.0855]]^{\frac{1}{2}} = 7.76''$$

Calibration of the Force Measurement Component

The force measuring component was calibrated in the configuration given in Figure 6 by means of attaching calibrated weights (1 to 10 lb). Under no load conditions, the recorder amplifier was balanced after a 30 minute warm-up period to a mean reading. Weights were attached to obtain tension loads or compression loads. Input section No. 3 of the recorder amplifier was used at a gain setting of 80. The results of the calibration tests are reported in Appendix A.

SIMULATOR CONFIGURATION

The Cargo Transport Simulator is shown schematically in Figure 7. It consists of 6 main elements; a cable drive system, a rotary inertia component, a velocity feedback component, a subject restraint component, a force transducer, and a supporting structure. The lower portion of the simulator, including the subject restraint

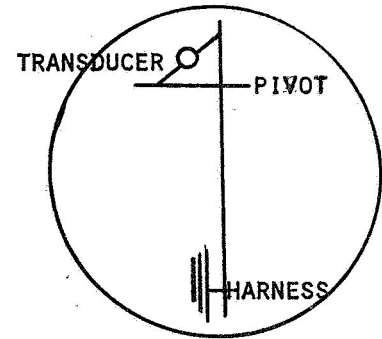
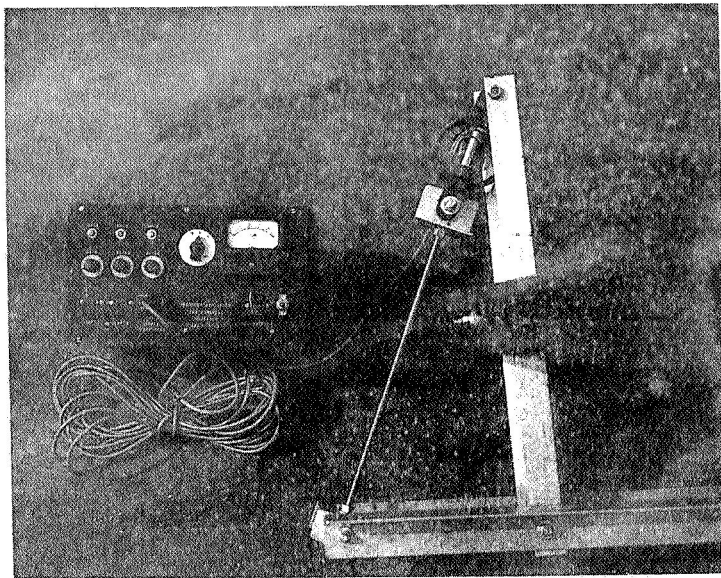


FIGURE 6 - FORCE MEASUREMENT COMPONENT

harness and the cable input section, is located below the water line while all other components are located outside the water.

The basic operation of the simulator takes advantage of the symmetric relative motion. Motions and forces occurring in cargo transport are simulated by the inertia of the rotational inertia component and linear translation of the cable. Since, for all practical purposes, the large space structures can be considered fixed in reference to small masses (astronaut carrying packages), and since we can, by change of point of reference, consider either element fixed relative to each other, the CTS fixes the subject and the package and permits relative motion of the spacecraft motion aid element.

In free space, the velocity of a cargo package will continue at a constant level if no forces are added. As a simple example, if an astronaut pushes a 1 slug mass with a force of 1 lb, he will accelerate the cargo at the rate of 1 ft/sec^2 , and if the 1 lb force is applied for 1 sec, the package will attain and maintain a velocity of 1 ft/sec if the package was originally at rest. The CTS provides these inertial motion characteristics by means of the velocity feedback component and the rotary inertia component

The CTS substitutes the rotational inertia of fixed masses located on its crossbar element for the linear inertia characteristics of the cargo. The current version of the CTS provides for approximately a 36:1 mass advantage, i.e., a 1 slug mass, located symmetrically on the crossbar, acts like 36 slugs, in linear translation. The velocity feedback element provides for undiminished motion of the simulated mass and overcomes linear resistance of the cable motion caused by water and rotary friction in the system.

Applied forces by the subject are measured by the force transducer which is located at the top of the subject restraint structure. The pivot action of the restraint structure causes input to the two-way force transducer. The subject motion is constrained by the threaded rod with gimbals at each end. The point of connection of the threaded rod to the restraint harness is adjusted to compensate for the combined mass of the subject and the cargo.

SIMULATION TECHNIQUE AND RESULTS

The simulation of cargo transport was performed by a trained scientist-subject, well versed in all aspects of water simulation, both pressure-suited and unsuited, who also had experience in the zero gravity research aircraft simulator. The subject evaluated cargo transport in the simulated weightless environment in an intravehicular mode, and was dressed in a standard short version of a SCUBA wet suit, ballasted to approximate neutral buoyancy by means of waist-mounted lead weights. Approximate neutral buoyancy is determined as the mean between neutral buoyancy at full inhale and exhale and is approximately ± 1 percent of neutral buoyancy. A continuous air supply is maintained by means of a HOOKAH arrangement configured to provide for minimum motion restriction.

The subject started the test by donning the restraint harness and adjusting the cable so that the cable was in the initial position. The subject was then handed one of the package configurations shown in Figure 8. The packages had approximate volumes of 1, 3.1, and 5.2 ft³, respectively. The preferential mode of carrying the packages was to place the subject's left arm through the two handles and carry the package as close to the body as possible,

Various other modes of carrying the packages were demonstrated during the program, including the package attached to the subject at waist level--two hands free, one-hand overhead carry, one-hand full extension of the arm to the left, foot carry, underarm carry, and between the legs carry. All of these modes appeared feasible, but offered various degrees of turning resistance and interference with cargo transport. This information was noted and documented by 35 mm slides for use in later stages of the program.

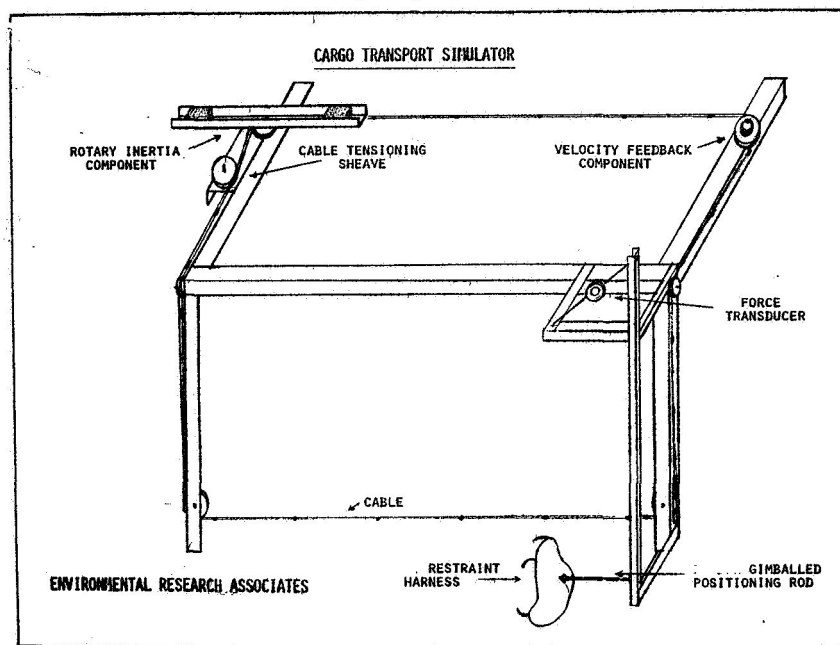


FIGURE 7 - CARGO TRANSPORT SIMULATOR SCHEMATIC

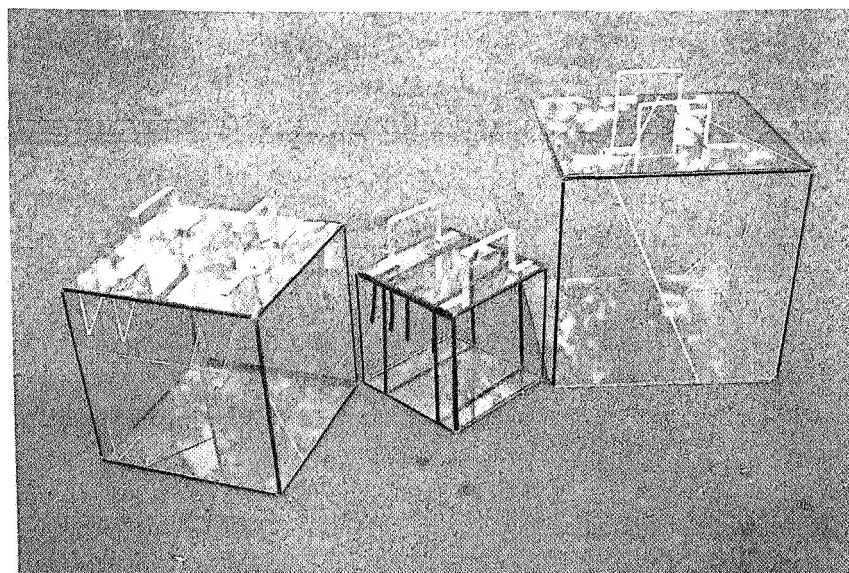


FIGURE 8 - CARGO CONFIGURATIONS

Additionally, a method of transporting the package along a suspended cable, not connected to the simulator, was evaluated for comparison purposes. The evaluation consisted of transporting the various dimensioned packages along a 1 in. diameter rope line suspended approximately 3 ft beneath the water line between two sides of the pool. The total travel length was approximately 30 ft.

This means of evaluating cargo transport does not appear to offer easily comparable data since the forces necessary to impart motion to the package are more than one order of magnitude greater than those required for package transport in space at reasonable velocities. Secondly, the motion of the subject and package are both subject to motion dependence and drag-planing effects. The velocity of the package is rapidly diminished by the drag of the water, but could, however, be mechanically compensated with a cable velocity feedback mechanism similar to that used in the (CTS).

The evaluation-research effort consisted of 18 test runs, comprising 9 package-mass configurations. The first 9 runs were performed by the subject prior to full familiarization with the action of the simulator. A second set of 9 runs was performed after a considerable indoctrination and familiarization period. Comparison between the first and second test series was indicative of learning characteristics. The simulated mass was adjusted to include both the 2, 6, and 10 slug package mass and the mass of the individual subject (5.3 slugs for subject 1 and 7 slugs for subject 2). Since the package geometries were constant (cubical package of volumes 1, 3.1, and 5.3 ft³, respectively), variation of the simulated masses was equivalent to variation of package density. Table I summarizes the 9 package-mass configurations.

TABLE I.--PACKAGE MASS - CONFIGURATION SUMMARY

CONFIGURATION				MASS*/SP. GRAV.		
				CENTROID		
DESIGNATION	SHAPE	DIMENSION	VOLUME	7.76"	10.73"	13.04"
1	CUBE	12" S	1	2/1	6/3	10/5
2	CUBE	17" S	3.1	2/0.3	6/1	10/1.7
3	CUBE	21" S	5.3	2/0.2	6/0.6	10/1

* slugs

The subject was instructed to don the restraint harness and grasp the cargo package by means of the two handles and carry the package in a comfortable manner. Each run consisted of transporting

the package along a simulated 31 ft linear path. Motion was started by the subject's grasping the transport cable with his right hand and applying force to the cable by a pulling motion. The cable was marked at 1 ft increments by a one-half in. band around the cable circumference. A 1 ft section was completely marked by an orange color. This section represented both the starting and finishing point.

The subject was instructed to accelerate and move the package at rates capable of control, and to decelerate and stop himself and the package precisely at the end of the orange-marked section. Photographic coverage was maintained throughout each test run. Manual or mechanical velocity feedback provided for continuation of the relative motion of the package-subject and the spacecraft transport component.

To initiate a test run, the subject reached forward, took hold of the cable in his right hand, and exerted a pulling force along the cable. Since this pulling force is composed of a component along and perpendicular to the cable and not directly in line with the intended direction of travel of the combined mass center, the subject must also exert continuous torque to prevent a yaw motion. The system mass center, being held at the ball joint, is restrained in the direction of travel, but has modified freedom in rotation and the other two directions. Therefore, the force exerted on the line results in motion around the mass center of the subject-cargo system and in rotational acceleration of the (RIC) which simulates the mass being transported.

The initial pulling stroke of the subject during a typical test run required approximately 1-1/2 sec, whereas the second stroke required slightly less than 1 sec, and further strokes continued at a rate of approximately 2/3 sec per stroke. In all tests, the subject accelerated the mass system to the resulting constant transfer velocity in about 3 sec, with a maximum of 3 strokes.

Motions in the yaw axis are discernable during this acceleration period, both in a clockwise and counterclockwise direction, throughout the test runs; the counterclockwise direction being the direction of motion predicted due to inertial effects. In several runs, there was a distinct yaw in the opposite direction as the subject compensated for this anticipated inertial motion.

During the constant velocity portion of the run, the subject continued to grasp the cable at approximately 36 in. increments, and used this hold on the cable to maintain a relative position. The subject had no apparent difficulty in maintaining this position nor in maintaining control of the handheld cargo. During this period, the line ran smoothly through the simulator system. The subject applied small forces against the cable to continually correct his position.

In order to decelerate the cable and the simulated mass, the subject exerted a semi-continuous counterforce on the cable. The force applied to the cable results in a relatively large magnitude yaw motion of the subject and cargo around the system mass center. Since the mass center is essentially fixed along the linear travel direction, this force decelerates the simulator-mounted inertia wheel, allowing the cable to come to a stop. The resulting body motion during the deceleration period was significantly different, depending on the height of the subject's center of mass in relation to the mean height of the cable. For example, if, at the point of initial deceleration, the subject carried the cable high, at the level of the upper torso, which implies that his center of mass was lower than the mean cable position, the resulting body motion consisted of a feet forward rotation about the mass center with an accentuation of the low mass center position. During runs when the subject decelerated with the mass center above the mean cable level, the resulting motion was an elevation of the mass center without the feet forward tendency. Decelerations, during which the initial position of the mass center was approximately at the mean cable level, were comparatively well controlled. In all cases, however, the subject was able to decelerate to a stop within a distance of 3 to 4 ft. Figure 9 presents an analysis of the linear motion of the subject-cargo during a typical run. This run utilized the 5.3 ft³ package with a simulated mass of 6 slugs. The total run of 33 ft took approximately 18 sec. The run was characterized by a period of rapidly

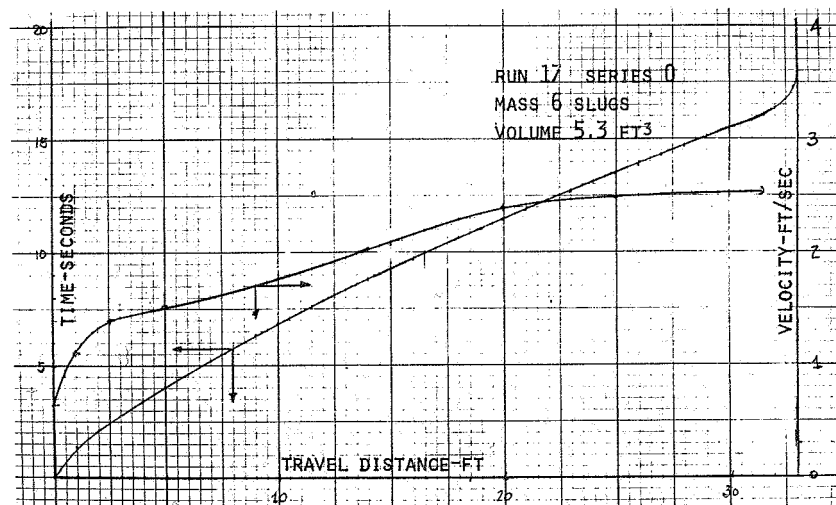


FIGURE 9 - MOTION ANALYSIS

increasing acceleration for approximately the first 5 ft of movement, after which there was a period of gradual acceleration to a maximum velocity of under 2.5 ft/sec during which the velocity was approximately constant. This was followed by an approximately 4 sec deceleration period during which linear and rotational body motion of the subject was stopped.

The subject was generally familiar with the simulation technique and the simulator. His experience in operating the simulator consisted of a series of checkout runs two days prior to the experimental tests. Learning characteristics were investigated by comparing experimental test series 1 and 2. For all package configurations, the second test series was accomplished in a shorter task time or at a greater velocity. It should be noted, however, that in the second series of runs, the subject exhibited an increased difficulty in arresting the package motion. This difficulty was accompanied by increased range and velocity of body motions. It appeared that the subject continually gained knowledge during the performance of the tests.

Tables II and III summarize the results of the final two series of cargo transport. Series 1 and 2 were identical in that they both comprised the 9 package masses identified in Table I. The primary difference between the two series is that series 1 was performed prior to the complete operational indoctrination of the subject.

The primary indicator of performance chosen for comparison was the average velocity of the maneuver. In the first series of tests, the subject exhibited considerable care in both accelerating the cargo and in decelerating the cargo. This caution resulted in fairly accurate control over the terminal position. The terminal position represents a fixed distance of approach to an assumed target. At these lower transport velocities, there appeared to be no significant effects resulting from mass or volume variation. The mean velocity of all runs of series 1 was 1.09 ft/sec.

During the second series, the average velocities were significantly higher for all runs. The mean average velocity for all runs of series 2 was 1.64 ft/sec. The subject exhibited a greater confidence in his abilities to control both the velocity and the acceleration of the mass. The results of this increased mean velocity were evidenced in a decreased accuracy of control of the terminal position of the maneuver with maximum overshoots of 2 ft. In all cases, the 31 ft travel limit was exceeded. It is reasonable to assume, however, that if proper visual feedback were introduced, that this overshoot could be reduced.

The subject increased his velocity by an average of 50 percent in the series 2 runs. This increase is directly due to familiarity

TABLE II.--RESULTS OF SIMULATION-SERIES 1

PACKAGE MASS-SLUGS	PACKAGE VOL-FT ³	SPECIFIC GRAVITY	AVERAGE VELOCITY FT/SEC
2	1.0	1.0	1.23
6	1.0	3.0	1.09
10	1.0	5.0	1.27
2	3.1	0.3	0.91
6	3.1	1.0	1.12
10	3.1	1.7	1.03
2	5.3	0.2	1.16
6	5.3	0.6	1.01
10	5.3	1.0	1.07

TABLE III.--RESULTS OF SIMULATION-SERIES 2

PACKAGE MASS-SLUGS	PACKAGE VOL-FT ³	SPECIFIC GRAVITY	AVERAGE VELOCITY FT/SEC
2	1.0	1.0	1.92
6	1.0	3.0	1.58
10	1.0	5.0	1.98
2	3.1	0.3	1.52
6	3.1	1.0	1.49
10	3.1	1.7	1.50
2	5.3	0.2	1.52
6	5.3	0.6	1.53
10	5.3	1.0	1.73

evidenced by repeated operations with the masses. The subject also exhibited greater amplitude on velocity motions during the deceleration phase. The magnitude of these motions was such that the package and subject could possibly have interacted with the target structure in real cases. The magnitude of this motion appears also to be sensitive to the lack of visual cues. As the velocity of transport increased, the subject appeared to start the deceleration phase too close to the end of travel, thus inducing the motions described.

Subject comment tends to support the premise that control of masses in a simulated weightless environment, while not being an inherently natural act, can be rapidly acquired through experience on the CTS simulator.

CONCLUSIONS AND RECOMMENDATIONS

The research effort under this program was constructed to achieve two major goals. The first was to demonstrate the operation of the Cargo Transport Simulator (CTS) concept and to provide first-order information to validate its utility. The second objective was to evaluate the cargo transfer operation of a subject in a simulated weightless, IVA mode, over a restricted range of cargo package masses and volumes. This range included cubical packages of 1, 3.1, and 5.3 ft³ and simulated masses of 2, 6, and 10 slugs. This yielded 9 package-mass combinations. In addition, a separate series of runs was accomplished to evaluate first-order learning characteristics.

During the performance of the program, several distinct versions of the CTS were developed, tested, and discarded for reasons stated in this report. The final version of the simulator incorporated a rotational inertia component and an endless cable to simulate the inertial effect of cargo motion in weightless conditions. Several improvements to this final system were conceived, but were not effected due to the scope of the program. These included automatic velocity feedback, computer-generated visual input, and variation of the motion aid element to include discrete handbars, continuous handrails, etc.

The operation of the simulator, in its present version, has successfully demonstrated the validity and utility of the CTS as a research device capable of broad utilization. The potential use of the CTS is not restricted to IVA operations. With minor modifications, the simulation technique can be used for both IVA and EVA cargo transfer investigations.

The results of the investigation of the transfer of the 9 package-mass variations indicate that manned, unassisted transport of packages within this range is not only feasible, but requires very

little training on the part of the subject for the IVA mode of transport. It is anticipated that inclusion of various other motion aid devices, such as continuous handrails, will also be easily accommodated, since the cable motion aid offers the least capability for force-torque transmissions.

There appears to be no major discernable difference in operation due to the different package-mass variations relative to time of transport or precision of operation. The subject's body motion was, however, visually different in the acceleration and deceleration phases. The result being that as package mass increased the acceleration phase was more deliberate and body motions during the deceleration phase exhibited increased amplitudes and velocities.

Further, the mode of body motion in the deceleration phase appeared to be determined by the relative position of the system barycenter and the mean level of the cable prior to the initiation of deceleration. This effect has not been fully investigated, however, and may be dependent on the simulator orientation, e.g., depend on the external gravitational field.

The motions during acceleration and deceleration were primarily functions of the package mass only, and did not appear to be affected by volume variations over the range of package masses considered in this investigation. The series of tests performed during this contract were particularly successful in showing the validity of the simulation to address the problem of cargo transport. The velocity profile of a typical test run follows an analytically predictable pattern for an astronaut carrying a relatively large package mass along a cable in weightlessness.

There are, however, a number of recommendations which would result in improved validity of the simulation. The major deficiency of the simulator was the absence of a technique to compensate for system friction. The result is that the subject found it harder to begin the motion of the simulated package mass, but found it easier to decelerate the package. In addition, he was required to continually compensate for the friction of the system during the period of travel. It is suggested that a servo-system can be adapted to the simulator which will measure the forces imparted to the line and compensate for the system friction, thereby increasing the fidelity of the overall simulation.

The point of attachment of the gimballed force transmission rod to the subject-mass combination was an approximation of the mass center of the subject mass. Additional effort is required to completely identify the position and motion of the system barycenter and to design a mechanism to compensate for the shift in position due to movement of the subject or mass. The length of the gimballed positioning rod which restrains the subject was approximately 18 in. It appeared as though this close coupling

may have provided erroneous stability to the test subject. It is recommended that a series of tests be performed, with varying lengths of positioning rod, for the purpose of identifying the effect of the rod length. Potentiometers, located at the terminals of the force transmission rod, could possibly be a means of direct measurement of the subject's motion.

The motion assist element investigated was a 5/16 in. braid-on-braid, white dacron cable. It consisted of a continuous line, spliced for uniformity, which was marked at 12 in. increments. One 12 in. section was colored orange. The orange section was preceded by a double section of black tape, 2 ft prior to the orange section. The test subject used the double mark and the orange section as a visual cue to his distance of travel. Future tests should include different diameters and types of cables, and should include a variety of marking procedures to investigate the test subject's control over the precision of the transfer maneuver.

The test subject, during these tests, was outfitted in SCUBA gear with a normal SCUBA mask. In this condition, the fidelity of the simulation is seriously affected by the visual cues. The subject is aware that he is moving a line through the water and not moving along the line. It is recommended that consideration be given to techniques of visual simulation, such as motion picture display, coordinated with line motion so as to give the subject a visual feedback indicating his approach to his stop position. There are a variety of techniques available in this area.

The simulated cargo packages used in the test series were constructed of plexiglass and balanced to neutral buoyancy when filled with water. The three sizes of cargo packages, therefore, determine three distinct masses of water controlled by the forces produced by the subject. Therefore, when the water drag is negligible, the packages exhibit three distinct inertial characteristics. The motion of the packages is reduced by the drag attendant on motion in the water. Previous studies have shown that these drag effects increase with velocity, but are negligible at less than 1/2 ft/sec. Observation of the package motion during the tests shows these velocities to be very low in all but the deceleration phase. The motion of the cargo around its own mass center is small and is, therefore, not affected by water drag, to any great degree.

The major limitation in the use of this type package is that the inertial properties transverse to the line of travel are fixed while the inertial reaction along the line of travel is variable, since the actual package density is equal to the density of water. It appears feasible that cargo with different mass densities can be simulated with the assistance of a cable support, attached to a gimbal at the mass center of the package. Position changes of

this mass are accomplished by means of a balance weight mounted on a swiveling sheave. In this manner, an evaluation of the total capability of a test subject to transport cargo in a controlled fashion can be made.

Environmental Research Associates feels that the results of this investigation have proven the value of the simulation technique. The application of this technique to anticipated space operation warrants an expanded program to investigate the critical portions of the simulation, and to provide data required by space designers for future space missions.

SYMBOLS

F_{ω}	weight component of force F, pounds
F_D	drag component of force F, pounds
F	force, pounds
W	weight, pounds
F_0	resultant friction force of the system, pounds
N	normal force, pounds
F_n	normal force, pounds
k	constant
m	mass, slugs
g	acceleration of gravity, feet/second ²
θ	angle
A	constant
ϕ	angle
R	mass centroid, feet
M	mass, slugs
I	moment of inertia, slug-feet ²
r_o	radius of the drive pulley, feet
α	angular acceleration, second ⁻²
a_{τ}	tangential acceleration, feet/second ²
m_s	simulated mass, slugs
I_T	total moment of inertia of the RIC, slug-feet ²
m_{s_e}	simulated mass (experimentally determined), slugs
m_o	mass-subject, slugs
m_p	mass-package, slugs
R_i	centroid of the i^{th} package, feet

APPENDIX A

DETERMINATION OF THE OPERATIONAL CHARACTERISTICS OF THE RIC

Description: Equipment setup and geometry as described in the main body of the report.

- Conditions:
- (1) No masses added to structure.
 - (2) Accelerating weight - 2.25#.
 - (3) Travel distance - 2.0 ft.
 - (4) Drive pulley radius - 2.063"

TABLE 1.--RESULTS OF CALIBRATION SERIES 1

RUN NO.	TRAVEL TIME (SEC)	$(X - \bar{X})^2$
1	2.160	0.0019
2	2.190	0.0002
3	2.220	0.0003
4	2.170	0.0012
5	2.230	0.0007
6	2.215	0.0001
7	2.245	0.0017
	Σ 15.430	0.0061
$\bar{X} - 2.204 \quad \sigma - 0.052$		

Therefore, the (1σ) travel time is 2.204 ± 0.052 sec.

Now, using the time for travel 2.204 ± 0.052 sec, the acceleration (a) is

$$a = 0.82 \pm 0.04 \text{ ft/sec}^2$$

The effective mass of the support structure for rotational inertial considerations is 2.75 ± 0.13 slugs.

During the first series of calibration runs, an anomaly in the suspension of the accelerating weight was observed. A second series of calibration runs was performed and is given in Table II.

- Conditions: (1) No masses added to structure.
 (2) Accelerating weight - 2.25#
 (3) Travel distance - 2 ft.
 (4) Drive pulley radius - 2.063".

TABLE II.--RESULTS OF CALIBRATION SERIES 2

RUN NO.	TRAVEL TIME (SEC)	$(x - \bar{x})^2$
1	2.275	.000060
2	2.270	.000009
3	*	--
4	2.270	.000009
5	*	--
6	2.270	.000009
7	2.265	.000009
8	2.260	.000049
9	2.270	.000009
10	2.262	.000025
11	2.265	.000004
12	2.262	.000025
	Σ 22.669	0.000208
	\bar{x} 2.262	σ - .0094

* hit/rebound

Therefore, the (1σ) travel time is 2.267 ± 0.0094 sec and the acceleration is 0.778 ± 0.007 ft/sec².

The effective mass of the support structure for rotational inertial considerations is 2.892 ± 0.026 slugs.

A series of runs was made to evaluate the resulting RIC configuration. The data from these runs is given in Table III.

TABLE III.--CALIBRATION RUNS WITH TEST MASS VARIATION

RUN NO.	WT. ADDED	ACC. WT.	CENTROID	DROP TIME	\bar{t}	DROP DISTANCE	PACK. MASS SLUGS
1	10#	1.25#	13.04"	7.211	7.715	2'	10
* 2	10	1.25	13.04	7.100		2	10
3	10	1.25	13.04	7.220		2	10
4	10	1.25	13.04	7.168		2	10
5	10	1.25	10.73	6.140	6.142	2	6
6	10	1.25	10.73	6.150		2	6
7	10	1.25	10.73	6.150		2	6
8	10	1.25	10.73	6.146		2	6
9	10	1.25	7.76	4.960	4.951	2	2
10	10	1.25	7.76	4.935		2	2
11	10	1.25	7.76	4.960		2	2
12	10	1.25	7.76	4.950		2	2
13	10	1.25	13.04	7.140	7.108	2	10
14	10	1.25	13.04	7.090		2	10
15	10	1.25	13.04	7.100		2	10
16	10	1.25	13.04	7.100		2	10

* discounted; changed method of drop to maintain constant tension in line; device wound up under 1.25# wt.

The resulting average accelerations and effective simulated masses are:

$$\bar{a}_1 = 0.163 \quad \bar{m}_{s_1} = 7.661 \text{ slugs}$$

$$\bar{a}_2 = 0.106 \quad \bar{m}_{s_2} = 11.787 \text{ slugs}$$

$$\bar{a}_3 = 0.079 \quad \bar{m}_{s_3} = 15.787 \text{ slugs}$$

Table IV presents the results of the initial calibration run of the RIC and provides an estimate of the friction force acting to retard the RIC.

TABLE IV.--RIC - INITIAL CALIBRATION RUN

TEST RUN	ADDED WT. (#)	CENTROID OF THE ADDED WT. (FT)	REFERENCE WT. (#)	DROP TIME-SEC. (355°-1.09')
1	4.5	1.11	1	4.412
2	4.5	1.11	2	3.120
3	0	--	2	1.560
4	64.4	1.05	1	11.910
5	64.4	1.05	1	11.750
6	--	--	0.032*	--

* Device moved with constant velocity.

The force measuring component was calibrated by the method described in the report, and the results of the calibration are given in Table V.

TABLE V.--FMC CALIBRATION

COMPRESSION LOADS			TENSION LOADS		
WEIGHT (#)	VOLTAGE (VOLTS)	CHANGE (VOLTS)	WEIGHT (#)	VOLTAGE (VOLTS)	CHANGE (VOLTS)
0	2.50	0	0	2.50	0
1	2.75	0.25	1	2.20	0.30
2	3.00	0.50	2	1.95	0.55
3	3.24	0.74	3	1.75	0.75
4	3.44	0.94	4	1.55	0.95
5	3.65	1.15	5	1.38	1.12
6	3.95	1.45	6	1.20	1.30
7	4.10	1.60	7	1.05	1.45
8	4.25	1.75	8	0.85	1.65
9	4.40	1.95	9	0.70	1.80
10	4.60	2.10	10	0.45	2.05

APPENDIX B

ANALYSIS OF FORCES FOR UW CARGO TRANSPORT SIMULATOR--LINEAR VERSION

In the linear version, the CTS would incorporate a sloped track along which a mass equal to the cargo mass would move. For a track sloped at an angle α , and for movement down the track, the geometry is given in Figure 1.

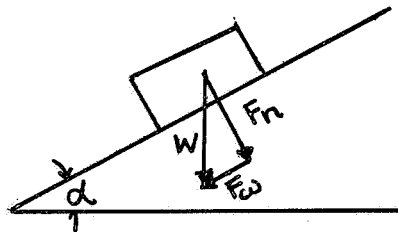


FIGURE 1 - TRACK GEOMETRY

The friction force resisting movement = $F_n k$, where k is the coefficient of friction and F_n is the normal force on the track.

For movement to occur,

$$F_i + F_w > F_n k$$

where F_i is the input force from the subject.

From the geometry of the problem,

$$F_w = W \sin \alpha$$

$$F_n = W \cos \alpha$$

Therefore, for $F_i = 0$, no slipping,

$$W \sin \alpha = W(\cos \alpha) k$$

The net force for motion down the track is

$$F_R = F_i + F_\omega - F_n k$$

since the friction acts in opposite sense to the motion.

For motion in the reverse direction,

$$F_R = F_i - F_\omega - F_n k$$

since the weight and friction forces act in the same direction.

Conclusions

For the same acceleration, one must exert a force of $2F_\omega$ greater for motion up the incline over motion down the incline. Therefore, it appears that the linear translation concept does not lend itself to continuous simulation of cargo transport since the provision to alternate the slope of the track in response to direction of force application would needlessly complicate the simulation.